Friend, not Foe: Lowered Tissue Reactivity to Long-Term Polyimide Implants

Corinne Orlemann[1], Laura M. De Santis[1], Paul Neering[1], Christian Boehler[2,3,4], Kirti Sharma[3,4], Arno Aarts[5], Tobias Holzhammer[5], Rik J.J. van Daal[5], Patrick Ruther[3,4], Maria Asplund[2,3,4,6], Roxana N. Kooijmans[1,7]*, Pieter R. Roelfsema[1,8,9,10]*

*Corresponding Authors

[1]Department of Vision and Cognition, Netherlands Institute for Neuroscience, Amsterdam, Netherlands
[2]Intelligent Machine-Brain Interfacing Technology (IMBIT), University of Freiburg, Freiburg, Germany
[3]Center BrainLinks-BrainTools, University of Freiburg, Freiburg, Germany
[4]Department of Microsystems Engineering (IMTEK), University of Freiburg, Freiburg, Germany
[5]ATLAS Neuroengineering BV, Leuven, Belgium
[6]Department of Microtechnology and Nanoscience, Chalmers University of Technology, Gothenburg, Sweden
[7]Forschungszentrum Jülich, INM-1, Jülich, Germany
[8]Sorbonne Université, Institut de la Vision, Paris, France
[9]Department of Integrative Neurophysiology, Vrije Universiteit Amsterdam, Amsterdam, Netherlands
[10]Department of Neurosurgery, Academic Medical Center, Amsterdam, Netherlands

Keywords

Neurotechnology, Biocompatibility, Histology, Intracortical electrodes, Foreign body response

Abstract

One of the biggest challenges for neurotechnology is the design of devices that are tolerated well by brain tissue, without sacrificing functionality and implantability. This study examined which design choices mitigate tissue damage and improve longevity, by varying probe features implanted in the cerebral cortex of mice.

We report on a systematic, quantitative analysis of neuronal and inflammation markers across cortical depth. We implanted a total of 103 stiff silicon or flexible polyimide probes in 32 mice, varying their thicknesses and widths, which were either attached to the skull or not. A new, automated workflow to quantify immunohistochemical data examines: 1) the tissue loss caused by the implant, 2) the cortical neuronal density, and 3) the immune response expressed by astrocytic and microglial reaction.

Flexible polyimide probes exhibited a clear advantage, with fewer lesions and weaker immune responses than stiff silicon probes. Furthermore, we observed a weaker influence of the shank cross-section. A cortical depth profile of immune reactivity revealed focal reactions at the device entry points in the superficial cortex and at the cortex-white matter boundary. This study gives important insights on optimizing device design parameters as well as surgical insights for improved tissue integration of intracortical electrode arrays.

Introduction

Over the past years the field of neurotechnology has seen a rapid advancement of technological developments for interfacing with the brain(Dalrymple et al., 2025; Vázquez-Guardado et al., 2020). One of the most reliable strategies is to implant microelectrode arrays into the brain, which can record brain signals at a high spatial and temporal resolution and stimulate neurons by delivering weak electrical currents. These neuronal probes have been successfully applied to read and write to the brain, retrieving motor commands from the brain of paralyzed individuals (Collinger et al., 2013; Hochberg et al., 2012) and generate sensations in prosthetic applications for touch and vision (Chen et al., 2020; Fernández et al., 2021; Flesher et al., 2016).

A main limitation of intracortical neuronal probes is their adverse effect on the targeted neuronal networks (Biran et al., 2007; Otte et al., 2022; Wellman et al., 2019; Woolley et al., 2013). Implantation requires advancing the probe through an opening in the skull and into the brain tissue, inherently damaging neurons and blood vessels along its path (Kook et al., 2016; Otte et al., 2022). The tissue reaction to an implanted foreign body is twofold (McConnell et al., 2009; Polikov et al., 2005; Szarowski et al., 2003). During the implantation, the probe ruptures the blood vessels and cuts through neuronal connections, triggering an initial acute inflammatory reaction. This reaction primarily consists of activated microglial cells responding to the injury and lasts about one to two weeks (Kozai et al., 2012; Potter et al., 2012). After this primary tissue response, a second, chronic inflammatory response occurs. This chronic reaction is characterized by the formation of scar tissue with reactive astrocytes along the electrode track and the loss of neurons around the site of implantation (Salatino et al., 2017). So far, the only commercially available devices are rigid silicon probes, like the Utah-array (Campbell et al., 1991; Obidin et al., 2020) and more recently, active stiff devices such as the Neuropixels (Steinmetz et al., 2021), the SiNAPS probe (Angotzi et al., 2019) or fully immersible probes as introduced by De Dorigo et al. (2018). Active devices minimize the space occupied by interconnection lines, substantially reducing the probe cross-section. Several studies report on the ability to record neuronal activity with these devices over months to years, but there is an invariable decline in device functionality over time (Barrese et al., 2013). The glial scarring and neuronal damage caused by the chronic inflammation is one of the major reasons quoted for the loss of functionality (Polikov et al., 2005; Szarowski et al., 2003). Reactive astrocytes form a sheath around the implant and replace the neurons near the electrodes, increasing the distance of the microelectrodes to the closest neurons they can record or stimulate. This adverse response decreases recording quality and increases currents necessary for electrical stimulation (Chen et al., 2023). In recent years, researchers and device manufacturers started to shift towards the use of highly flexible polymer-based

probes (Du et al., 2017; Lind et al., 2013; Luan et al., 2017; Nguyen et al., 2014; Park et al., 2021; Tian et al., 2023; Zhao et al., 2023), aiming to counteract the adverse effects of rigid silicon-based probes on the brain tissue. Due to their flexibility, these probes can follow the movements of the brain tissue, and the material allows the fabrication of thinner probes that do not break when implanted into the brain. Several studies have reported high functionality of such devices, which can record brain signals over a long period of time and stimulate neurons with low currents (Chung et al., 2019; Lycke et al., 2023; Orlemann et al., 2024; Yasar et al., 2024).

Previous studies examined how the size of the probes and the surgical implantation strategy influence how well they integrate in the brain tissue. Bulkier probes replace more tissue and cause more neuronal damage than probes of smaller size (Seymour & Kipke, 2007; Stice et al., 2007; Thelin et al., 2011), and in case of flexible probes, thicker probes are more rigid than thinner ones. Furthermore, silicon probes can be pushed into the brain because they are rigid, but polyimide probes are most often inserted using shuttle devices, which are retracted upon implantation so that only the flexible probe stays behind. The insertion of these shuttle devices inevitably increases the implantation footprint, causing additional tissue loss (Otte et al., 2022).

The connection between the probe and the connector plays another important factor in the development of neural devices. Many current devices are tethered; the brain implant is connected to a fixed position, e.g. a printed circuit board (PCB) on the skull. Prior studies have shown that this tethering can induce additional chronic trauma to the brain, presumably because it limits the ability of the probe to follow the micromovements of the brain (Biran et al., 2007; Kim et al., 2004; Thelin et al., 2011; Vomero et al., 2022).

Despite rapid advancements in neurotechnology, it is still uncertain which design parameters play the most important role in promoting tissue integration. While the consensus is that higher flexibility aids longevity, the trade-offs between material and dimensions of the probe and the best implantation technique remain uncertain. How does the damage caused by a silicon probe of minimal cross-section compare to that caused by a polyimide probe that is larger to harbor enough microelectrodes? Many of the forementioned studies addressed some of the sub-questions about device design in isolation, but, to our knowledge, no previous study directly compared the tissue compatibility of flexible and rigid electrode arrays of various widths and thickness that were either tethered or free floating. Knowledge about the relative influences of these factors on implant longevity will be essential for the future design choices for biocompatible brain implants.

We here present a comprehensive dataset of over a hundred brain slices collected from mice implanted with polyimide or silicon probes of various cross-sections, using either a tethered or untethered design. We developed a new quantitative histological analysis pipeline to investigate tissue reactions based on the presence of neurons, astrocytes, and microglia.

Furthermore, we investigated the reaction along the entire probe, examining the cortical depth profile and underlying white matter. We observe a depth dependent immune response for all probes and report a general advantage of the flexible polyimide probes on tissue integrity, accompanied by weaker influences of other design parameters like probe dimensions.

Results

We examined the influence of probe material, geometry, and implantation strategy on long-term tissue responses in the cortex of mice. We implanted rigid silicon probes and flexible polyimide probes that varied in shank width (35, 70, and 105 µm) and thickness (polyimide: 2, 5, 15 or 25 µm; silicon: 15, 25 or 50 µm), which were either tethered to the skull or left untethered. The probes had a comb-like design, consisting of three parallel shanks of identical thickness but different widths (Figure 1A-D). Many probes did not have functional electrodes because our main goal was to examine the tissue effects, but we also implanted probes with functional electrodes to assess recording quality over time. In total, 32 mice were implanted with three or four comb-like probes (i.e. a total of 9 to 12 shanks, Figure 1C), of which 30 mice were examined after approximately 6 months and two after 12 months of implantation. We inserted the probes with stereotaxic guidance, and we used temporary shuttle devices, which were retracted after insertion, to deliver the flexible probes. Tethered probes had wings that we attached to the skull with cement, and we placed untethered probes under a stainless-steel cap with a high inner roof that replaced a piece of the skull to prevent pressure from the skull onto the probes (Figure 1B). After the implantation period, we sacrificed and perfused the mice, sectioned their brains, and processed the sections for quantitative histology, recovering hundreds of probe shank tracks across the mice. We noticed that some of the shanks gave rise to loss of cortical tissue and quantified these lesions. Our histological analysis focused on neuronal density (NeuN), astrocytic reactivity (GFAP) and microglial activation (IBA1) (Figure 1C,D). In what follows, we will first quantify gross lesions caused by the probes in several mice. We will then characterize the immune responses across the cortical depth, the neuronal and glial reactions to the design parameters, the effects of implantation duration, and finally the relationship between tissue integration and the electrophysiological recording stability.

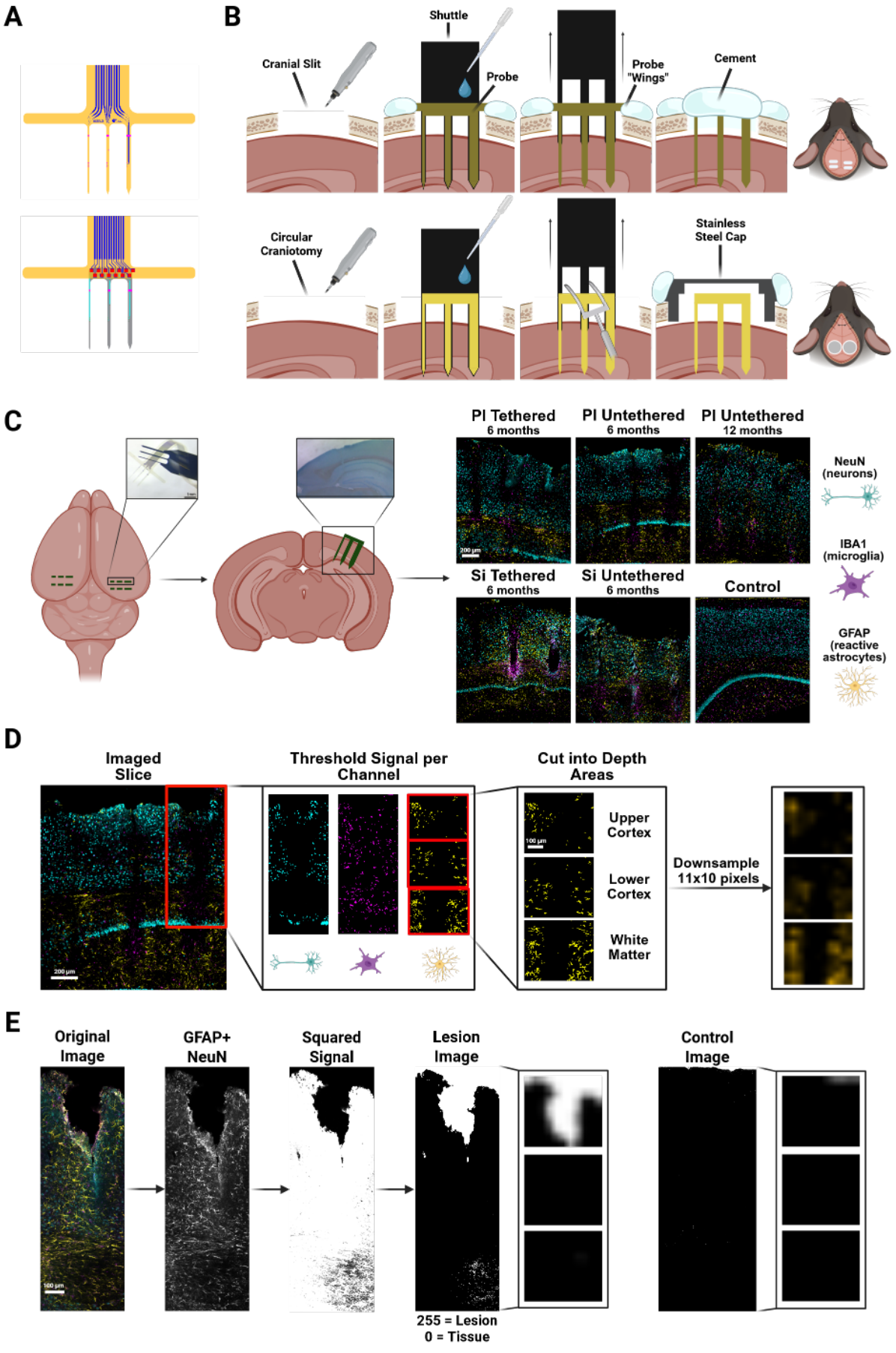

FIGURE 1. Implantation approach and quantification of the effects on the cortex. **(A)** Probe designs.

Each probe consisted of 3 shanks of three different widths: 35, 70, and 105 µm and had one of several thicknesses. Polyimide probes (top) had a thickness of 2, 5, 15 or 25 µm and silicon probes (bottom) a thickness of 15, 25 or 50 µm. **(B)** Surgical procedures. We implanted 3-4 probes, with three shanks each in each mouse. Top: Tethered polyimide probes were inserted with a shuttle device after drilling a cranial slit of 1.5 mm into the mouse skull. The probes had wings that were attached to the skull with cement. The shuttle was removed and the craniotomy was sealed with cement. Bottom: Untethered polyimide probes were also inserted with a shuttle device. The probe detachment was supported with the help of a custom-made fork-like tool. A stainless-steel cap with a high inner roof was placed over the craniotomy and secured with cement. Silicon probe implantations followed the same procedure but did not require a shuttle device. **(C)** Immunohistochemistry. We sacrificed the mice after 6 or 12 months. We identified the lesions with Evan's Blue (marking albumin) and identified neuronal density with NeuN, microglia with IBA1, and reactive astrocytes with GFAP. Right: Example images of tethered and untethered polyimide (PI) and silicon (Si) probes and a control image. Scale bar = 200 µm. **(D)** Quantification pipeline. We identified neurons, astrocytes, and microglia around each probe shank in three ROIs: Upper cortex, lower cortex and white matter. Scale bars represent either 200 or 100 µm. **(E)** We also identified regions with loss of cortical tissue and quantified the extent of the lesions. Right: example control image. Scale bar = 100 µm.

Rigid probes cause more cortex loss

Several probes caused a loss of tissue, creating regions without cells (Figure 1E shows an example lesion). To quantify the tissue loss, we created binarized images of tissue vs. non-tissue (see Methods; Figure 1E). In short, we combined NeuN and GFAP fluorescence images and classified pixels as cortex or non-cortex. We then averaged the images per probe type and measured a normalized measure of tissue loss compared to unimplanted cortex, which we will call ΔTissueLoss. Higher values of ΔTissueLoss imply more tissue loss than control cortex (see Methods).

When we averaged across the entire depth profile, the tissue loss was more prominent for silicon probes than for polyimide probes (z = 4.21, p < .0001, N_{images} = 400; Figure 2A). To account for differences in tissue reactivity and tissue stress along the probe trajectories, we defined three regions of interest (ROIs): (i) the upper cortex, (ii) the lower cortex and (iii) underlying white matter (Methods). Each ROI extended approximately 460 µm in depth and 400 µm in the horizontal direction. The upper cortical ROI started at the pial surface and included the superficial cortical layers, which are more directly affected by probe entry and disruption of the meninges than the lower cortex. The middle ROI comprised the deeper cortical layers. It was aligned on the white matter boundary and extended in the direction of the pia. The lowest ROI began at the cortical–white matter boundary and extended downward, only including white matter. These three ROIs are central to our quantification approach and will be used in the rest of the analysis.

Tissue loss was more pronounced in upper cortex than in the lower cortex (z = -12.8, p< .0001, N = 282) and the white matter (z = -11.9, p < .0001, N = 269; Figure 2B). We next examined the probe design parameters within the three ROIs (Figure 2C). In the upper cortex, untethered silicon probes caused more tissue loss than tethered polyimide (z = 6.88, p < .0001, N = 77), untethered polyimide (z = 4.56, p < .0001, N = 70) and tethered silicon probes (z = 2.98, p

< .05, N = 72). Additionally, tethered silicon probes caused more tissue damage than tethered polyimide probes (z = 3.94, p < .001, N = 81). In the lower cortex, tethered polyimide probes caused the least amount of tissue loss, significantly less than tethered (z = 4.44, p < .0001, N = 61) and untethered silicon probes (z = 2.89, p < .05, N = 63). Tethered silicon probes also caused a loss of white matter, and more so than tethered polyimide probes (z = 3.61, p < .01, N = 51). To summarize, the probe material was a prime determinant of tissue loss, with silicon probes causing more damage than polyimide probes.

The width of the probe shanks also influenced the degree of tissue loss in the cortical ROIs (upper cortex: $\chi^2(2) = 14.76$, p < .001; lower cortex: $\chi^2(2) = 6.53$, p < .05). The 105 µm-wide shank caused more tissue loss than the 35 µm-wide shank in the upper (z = -3.45, p < .01, N = 98) and lower cortex (z = -2.55, p < .05, N = 80). Additionally, the 70 µm-wide shank caused more tissue loss than the 35 µm-wide shank in the upper cortex (z = -3.2, p < .01, N = 103; Figure 2D). We did not find significant effects of probe thickness on tissue loss.

We note, however, that tissue damage can also express as a more diffuse loss of neurons without a complete disruption of the cortex. We therefore quantified the density of remaining neurons with a NeuN stain. Figure 2E provides a first impression of how different probe types cause a decrease in neuronal density across cortical depth. Specifically, we converted the NeuN fluorescence images (Figure 1C,D) into quantitative profiles by creating a binary categorization of neurons in the image and down sampled the images to generate pixel wise representations along the probe track (see Methods). We then averaged the pixels across images in each condition. We will first describe the equivalent quantification for GFAP and IBA1 stains that measure the increases in astrocytic and microglia reactivity, before we return to the full quantification of the NeuN results, in a later section of the Results.